CRYSTAL GROWTH & DESIGN

Article

pubs.acs.org/crystal

# The First Observation of One-Dimensional Naphthalenediimidato-Based Transition-Metal Coordination Polymers: Syntheses, Crystal Structures and Properties

Tao Tao, Yan-Hua Lei, Yu-Xin Peng, Ying Wang, Wei Huang,* Zhao-Xu Chen,* and Xiao-Zeng You

State Key Laboratory of Coordination Chemistry, Key Laboratory of Mesoscopic Chemistry of MOE, Nanjing National Laboratory of Microstructures, School of Chemistry and Chemical Engineering, Nanjing University, Nanjing 210093, P. R. China

Supporting Information

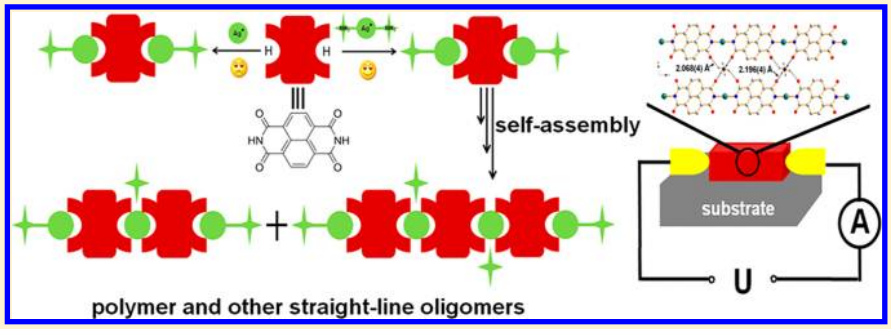


**ABSTRACT:** Metal-directed assembly of naphthalene-1,4,5,8-tetracarboxylic acid (NTA) with different transition-metal salts in the presence of ammonia results in a series of one-dimensional metal−naphthalenediimidato (M−NDI) coordination polymers with the formulas of $\{[Ag(NDI)](NH_4)\}_n$ (**P1**), $[Zn(NDI)(NH_3)_2]_n$ (**P2**), $[Cd(NDI)(NH_3)_2]_n$ (**P3**), $[Co(NDI)(NH_3)_2]_n$ (**P4**) and $[Ni(NDI)(NH_3)_2]_n$ (**P5**), respectively. It is worthwhile to mention that the 1D straight-line NDI−Ag(I) coordination polymer **P1** is formed stepwise from a dinuclear NDI−Ag(I) intermediate $[Ag_2(NDI)(NH_3)_2]$ (**2AgNDI**), where ammonia serves as a stabilizing reagent of Ag(I) ion and a weak base to remove the protons of $NDIH_2$ simultaneously. Furthermore, **P1** exhibits semiconducting properties in the solid state which may originate from its all-parallel-aligned packing structure (AAAA) which is different from the common ABAB packing mode for **P2**−**P5** and **2AgNDI**. In addition, theoretic computational studies as well as X-ray photoelectron spectrometer spectra on **P1** and **2AgNDI** have also been carried out.

## INTRODUCTION

Research on supramolecular chemistry, for instance, the constitution of one-dimensional (1D) metal coordination polymers (MCPs), has attracted considerable attention in recent years, not only because of their various and intriguing self-assembly structures but also owing to their interesting physical and chemical properties for research purposes and technical applications.[1] In addition, some complexes have been used in supramolecular electronics and nanosized optoelectronic devices to replace the metal and silicon-based materials in semiconducting devices such as molecular wires, field-effect transistors, photovoltaic devices, flat panel displays, light-emitting diodes, logic gates and so on.[2] For example, hundreds of metal organic rods based on alkynes have been described and demonstrated by the groups of Vivian Wing-Wah Yam[3] and Elena Lalinde.[4]

As is well-known, one of the most important problems is how to design or re-elect suitable organic ligands to rationally prepare MCPs on the basis of self-assembly. In past decades, aromatic *N*,*N*′-di(4-pyridyl)-1,4,5,8-naphthalenetetracarboxydiimide (DPNDI) and its derivatives were used as the bridging ligands to construct a variety of MCPs.[5] However, these building blocks are not planar because of the steric effects (Scheme 1). It is generally believed that increasing the planarity, which could reduce the reorganization energy and enhance the electronic coupling between adjacent molecules, would be much more efficient than distorted stacking for the transportation of charge carriers.[6] Considering the above-mentioned points, we simplify the chemical stucture of DPNDI and choose the naphthalene diimide, the derivatives of which are neutral, planar, chemically robust, redox-active compounds usually with high melting point and n-type charge mobility.[7] It is an ideal supramolecular building block to explore the self-assemblies of versatile $\pi$-conjugated systems on the 1−100 nm length scale (Scheme S1 in the Supporting Information).[8]

In our previous work, a series of p-type heterocyclic aromatic compounds (for instance, phenyl, imidazole, thiophene and oligothiophene groups) have been successfully introduced to 3,8-dibromo-1,10-phenanthroline and dibromothiophene systems.[9] Furthermore, temperature-dependent semiconducting and photoresponsive properties of self-assembled nanocomposite films and nanodevices fabricated from these compounds

**Received:** June 7, 2012
**Revised:** July 10, 2012
**Published:** July 11, 2012

   dx.doi.org/10.1021/cg300776y | *Cryst. Growth Des.* 2012, 12, 4580−4587

**Scheme 1. Structural Design of 1D Coordination Polymer from DPNDI Complex to NDI Complex**

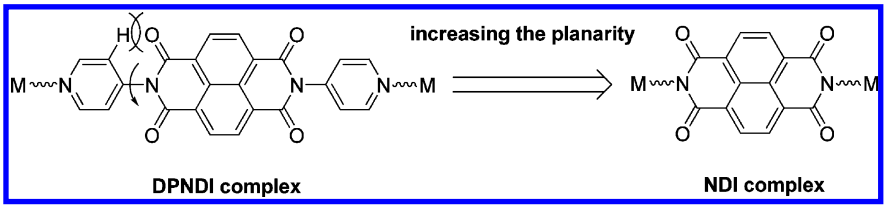


**Scheme 2. Schematic Illustration for the Preparation of Complexes P1−P5 Where the Different Coordination Configurations of Ammonia or Uncoordinated Ammonium Are Shown**

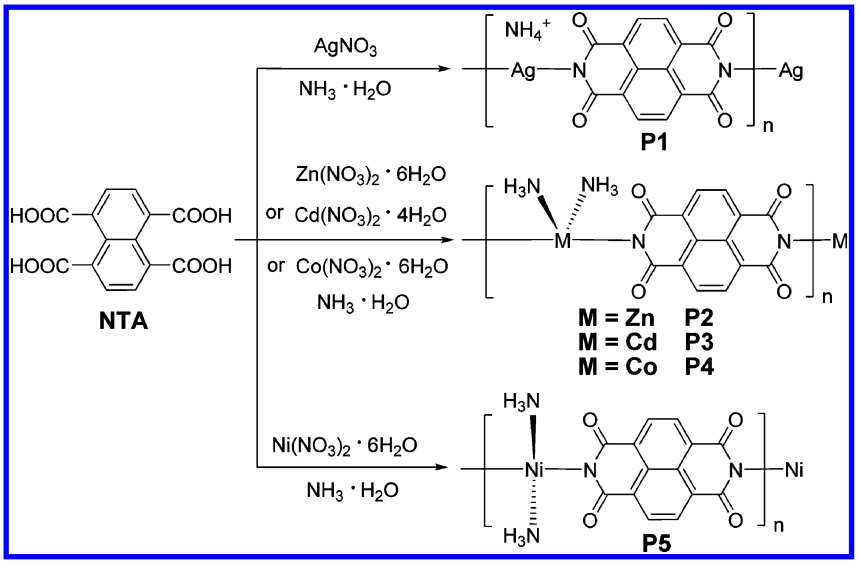


and their metal complexes have been explored.[10] However, the study of metal complexes with functionalized naphthalenediimidato linkers is not reported yet. Surprisingly, in view of the relatively fewer investigations on imidato-coordinated complexes,[11] we report herein five new linear naphthalenediimidato-based MCPs (Scheme 2), formulated as $\{[Ag(NDI)](NH_4)\}_n$ (**P1**), $[Zn(NDI)(NH_3)_2]_n$ (**P2**), $[Cd(NDI)(NH_3)_2]_n$ (**P3**), $[Co(NDI)(NH_3)_2]_n$ (**P4**) and $[Ni(NDI)(NH_3)_2]_n$ (**P5**). It is worth noting that we describe an unusual 1D straight-line NDI−Ag(I) coordination polymer **P1** formed stepwise from a dinuclear NDI−Ag(I) intermediate $[Ag_2(NDI)(NH_3)_2]$ (**2AgNDI**) in the presence of ammonia. To the best of our knowledge, this is the first structural report on the preparation and structures of metal−naphthalenediimidato complexes, wherein all the NDI units in **P1** are fully parallel in both its polymeric and packing structures showing a small band gap of 1.72 eV calculated by the density functional theory combined with ultrasoft pseudopotentials.

## EXPERIMENTAL SECTION

**Materials and Physical Measurements.** The reagents of analytical grade were purchased from commercial sources and used without any further purification. Elemental analyses for carbon, hydrogen and nitrogen were performed on a Perkin-Elmer 1400C analyzer. Infrared (IR) spectra (4000−400 $cm^{-1}$) were recorded using a Nicolet FT-IR 170X spectrophotometer on KBr disks. Powder X-ray diffraction (PXRD) measurements were performed on a Philips X'pert MPD Pro X-ray diffractometer using Cu K$\alpha$ radiation ($\lambda$ = 0.15418 nm), in which the X-ray tube was operated at 40 kV and 40 mA at room temperature. X-ray photoelectron spectrometer (XPS) determination was carried out by a Thermo Scientific K-Alpha system, where a monochromatic Al K$\alpha$ X-ray source was used with a spot area of 400 $mm^2$.

**Synthetic Procedures.** *Syntheses of $\{[Ag(NDI)](NH_4)\}_n$ (**P1**) and $[Ag_2(NDI)(NH_3)_2]$ (**2AgNDI**).* A mixture of $NH_3{\cdot}H_2O$ (5 mL), NTA (152 mg, 0.5 mmol), $AgNO_3$ (187 mg, 1.1 mmol) and 5 mL of distilled water was stirred together for 10 min and then tuned to pH = 9.5 with $NH_3{\cdot}H_2O$. After the ultrasonic processing of 5 min, the mixture was transferred into a 25 mL Teflon-lined stainless steel reactor and heated at 140 °C for 3 days under autogenous pressure. Then the autoclave was cooled to 100 °C at a rate of 10 °C·$h^{-1}$, held for 12 h and further cooled to room temperature at a rate of 5 °C·$h^{-1}$. Dark-orange crystals of **P1** and light-orange crystals of **2AgNDI** were obtained by manual separation with the yields of 14% (27.3 mg, based on NTA) and 47% (120.8 mg, based on NTA), respectively. **P1**: elemental analysis (%), anal. calcd for $C_{14}H_8AgN_3O_4$, C, 43.10; H, 2.07; N, 10.77; found, C, 42.84; H, 2.31; N, 10.63; main FT-IR absorptions (KBr pellets, $cm^{-1}$), 3405 (b), 1641 (s), 1569 (s), 1417 (m), 1384 (m), 1306 (s), 1185 (m), 952 (w), 874 (w), 771 (m), 565 (m), 439 (w). **2AgNDI**: elemental analysis (%), anal. calcd for $C_{14}H_{10}Ag_2N_4O_4$, C, 32.71; H, 1.96; N, 10.90; found, C, 32.53; H, 2.24; N, 10.72; main FT-IR absorptions (KBr pellets, $cm^{-1}$), 3406 (b), 2372 (w), 2061 (w), 1641 (s), 1570 (s), 1417 (m), 1384 (m), 1307 (s), 1188 (m), 1050 (m), 952 (w), 875 (w), 771 (m), 716 (w), 567 (m), 442 (w).

*Syntheses of Complexes **P2**−**P5**. $[Zn(NDI)(NH_3)_2]_n$ (**P2**).* The procedure for the synthesis of **P1** was repeated except that $Zn(NO_3)_2{\cdot}6H_2O$ (327 mg, 1.1 mmol) was used instead of $AgNO_3$ (187 mg, 1.1 mmol). Yield: 61% based on NTA. Elemental analysis (%): anal. calcd for $C_{14}H_{10}N_4O_4Zn$, C, 46.24; H, 2.77; N, 15.41; found, C, 45.96; H, 2.97; N, 15.25. Main FT-IR absorptions (KBr pellets, $cm^{-1}$): 3743 (w), 3455 (b), 3173 (w), 3073 (w), 2853 (w), 2359 (w), 1682 (s), 1569 (m), 1431 (m), 1338 (m), 1255 (s), 1087 (m), 861 (m), 761 (m), 617 (m).

*$[Cd(NDI)(NH_3)_2]_n$ (**P3**).* The above procedure was repeated using $Cd(NO_3)_2{\cdot}4H_2O$ (339 mg, 1.1 mmol) as the metal source. Yield: 76% based on NTA. Elemental analysis (%): anal. calcd for $C_{14}H_{10}CdN_4O_4$, C, 40.95; H, 2.45; N, 13.64; found, C, 40.71; H, 2.69; N, 10.48. Main


dx.doi.org/10.1021/cg300776y | Cryst. Growth Des. 2012, 12, 4580−4587

Table 1. Crystal Data and Structure Refinement Details for 2AgNDI and P1−P5[a]

| | 2AgNDI | P1 | P2 | P3 | P4 | P5 |
|---|---|---|---|---|---|---|
| empirical formula | $C_{14}H_{10}Ag_2N_4O_4$ | $C_{14}H_8AgN_3O_4$ | $C_{14}H_{10}N_4O_4Zn$ | $C_{14}H_{10}CdN_4O_4$ | $C_{14}H_{10}CoN_4O_4$ | $C_{14}H_{10}N_4NiO_4$ |
| formula wt | 514.00 | 390.10 | 363.65 | 408.65 | 357.19 | 356.95 |
| $T$ [K] | 291(2) | 291(2) | 291(2) | 291(2) | 291(2) | 291(2) |
| wavelength/Å | 0.71073 | 0.71073 | 0.71073 | 0.71073 | 0.71073 | 0.71073 |
| cryst size (mm) | 0.08 × 0.10 × 0.24 | 0.10 × 0.12 × 0.18 | 0.10 × 0.10 × 0.14 | 0.10 × 0.10 × 0.14 | 0.08 × 0.10 × 0.12 | 0.10 × 0.12 × 0.14 |
| cryst syst | monoclinic | triclinic | orthorhombic | orthorhombic | orthorhombic | orthorhombic |
| space group | $C2/c$ | $P\bar{1}$ | $Pnma$ | $Pnma$ | $Pnma$ | $Pbam$ |
| $a$ [Å] | 25.96(2) | 3.7843(8) | 9.8973(7) | 9.8973(7) | 9.9006(14) | 5.3699(8) |
| $b$ [Å] | 3.732(3) | 7.7515(16) | 21.2813(15) | 21.2813(15) | 21.354(3) | 10.6670(17) |
| $c$ [Å] | 15.585(14) | 10.297(2) | 6.2306(5) | 6.2306(5) | 6.2260(9) | 10.8909(17) |
| $\alpha$ [deg] | 90 | 92.957(2) | 90 | 90 | 90 | 90 |
| $\beta$ [deg] | 110.502(11) | 95.118(3) | 90 | 90 | 90 | 90 |
| $\gamma$ [deg] | 90 | 92.835(3) | 90 | 90 | 90 | 90 |
| $V$ [Å$^3$] | 1414(2) | 300.00(11) | 1312.34(17) | 1312.34(17) | 1316.3(3) | 623.84(17) |
| $Z/D_{calcd}$ (g/cm$^3$) | 4/2.415 | 1/2.159 | 4/1.841 | 4/2.068 | 4/1.802 | 2/1.900 |
| $F$(000) | 992 | 192 | 736 | 800 | 724 | 364 |
| $\mu$ [mm$^{-1}$] | 2.799 | 1.705 | 1.901 | 1.693 | 1.333 | 1.586 |
| max/min transmission | 0.8071/0.5531 | 0.8480/0.7489 | 0.8327/0.7767 | 0.8490/0.7975 | 0.9009/0.8564 | 0.8575/0.8085 |
| $h_{min}/h_{max}$ | −30/18 | −4/4 | −12/6 | −10/12 | −12/13 | −6/7 |
| $k_{min}/k_{max}$ | −4/4 | −9/8 | −26/26 | −26/26 | −24/28 | −13/14 |
| $l_{min}/l_{max}$ | −16/18 | −12/11 | −7/7 | −7/5 | −8/6 | −11/14 |
| data/params | 1247/110 | 1054/103 | 1327/123 | 1327/109 | 1659/109 | 796/58 |
| final $R$ indices | R1 = 0.0348 | R1 = 0.0304 | R1 = 0.0287 | R1 = 0.0230 | R1 = 0.0477 | R1 = 0.0363 |
| [$I > 2\sigma(I)$] | wR2 = 0.0837 | wR2 = 0.0658 | wR2 = 0.0697 | wR2 = 0.0554 | wR2 = 0.0542 | wR2 = 0.0806 |
| $R$ indices | R1 = 0.0418 | R1 = 0.0332 | R1 = 0.0355 | R1 = 0.0278 | R1 = 0.1231 | R1 = 0.0499 |
| (all data) | wR2 = 0.0871 | wR2 = 0.0827 | wR2 = 0.0722 | wR2 = 0.0571 | wR2 = 0.0651 | wR2 = 0.0856 |
| $S$ | 0.957 | 1.166 | 1.017 | 1.056 | 0.701 | 0.969 |
| max/min$\Delta\rho$ [e·Å$^{-3}$] | 0.71/−0.86 | 0.49/−0.72 | 0.33/−0.53 | 0.34/−0.69 | −0.71/−0.49 | −0.42/−0.58 |

[a] $R1 = \sum||F_o| - |F_c||/\sum|F_o|$, $wR2 = [\sum[w(F_o^2 - F_c^2)^2]/\sum w(F_o^2)^2]^{1/2}$.

FT-IR absorptions (KBr pellets, cm$^{-1}$): 3367 (b), 1650 (vs), 1575 (vs), 1437 (m), 1381 (m), 1312 (vs), 1180 (m), 1112 (m), 780 (m), 623 (m).

*$[Co(NDI)(NH_3)_2]_n$ (**P4**).* The above procedure was repeated using $Co(NO_3)_2·6H_2O$ (320 mg, 1.1 mmol) as the metal source. Yield: 46% based on NTA. Elemental analysis (%): anal. calcd for $C_{14}H_{10}CoN_4O_4$, C, 47.08; H, 2.82; N, 15.69; found, C, 46.82; H, 3.04; N, 15.53. Main FT-IR absorptions (KBr pellets, cm$^{-1}$): 3448 (b), 3173 (m), 3073 (m), 2853 (m), 1707 (vs), 1676 (vs), 1575 (s), 1444 (m), 1344 (s), 1262 (s), 867 (m), 761 (m), 623 (m).

*$[Ni(NDI)(NH_3)_2]_n$ (**P5**).* The above procedure was repeated using $Ni(NO_3)_2·6H_2O$ (320 mg, 1.1 mmol) as the metal source. Yield: 39% based on NTA. Elemental analysis (%): anal. calcd for $C_{14}H_{10}N_4NiO_4$, C, 47.11; H, 2.82; N, 15.70; found, C, 46.97; H, 3.02; N, 15.55. Main FT-IR absorptions (KBr pellets, cm$^{-1}$): 3429 (b), 1701 (vs), 1680 (vs), 1616 (vs), 1577 (m), 1487 (w), 1438 (m), 1346 (m), 1271 (s), 1098 (vs), 1020 (m), 920 (w), 835 (m), 764 (w), 623 (s), 518 (m), 428 (m).

**X-ray Data Collection and Structural Determination.** Single-crystal samples of complexes **2AgNDI** and **P1−P5** were glue-covered and mounted on glass fibers for data collection on a Bruker SMART APEX CCD diffractometer using graphite monochromated Mo K$\alpha$ radiation ($\lambda$ = 0.71073 Å) at room temperature. The collected data were reduced by using the program SAINT,[12] and empirical absorption corrections were done by the SADABS[13] program. The crystal systems were determined by Laue symmetry, and the space groups were assigned on the basis of systematic absences by using XPREP. The structures were solved by direct method and refined by least-squares method. All non-hydrogen atoms were refined on $F^2$ by full-matrix least-squares procedure using anisotropic displacement parameters, while hydrogen atoms were inserted in the calculated positions assigned fixed isotropic thermal parameters at 1.2 times the equivalent isotropic $U$ of the atoms to which they are attached and allowed to ride on their respective parent atoms. All calculations were carried out on a PC with the SHELXTL PC program package,[14] and molecular graphics were drawn by using XSHELL, Diamond and ChemBioDraw softwares. Details of the data collection and refinement results for **2AgNDI** and **P1−P5** are listed in Table 1, while selected bond distances and bond angles are given in Table 2. Moreover, intermolecular N−H···O hydrogen bonding interactions are given in Table S1 in the Supporting Information.

## RESULTS AND DISCUSSION

**Structural Descriptions of $\{[Ag(NDI)](NH_4)\}_n$ (P1) and $[Ag_2(NDI)(NH_3)_2]$ (2AgNDI).** The pure phase of **P1** and **2AgNDI** is confirmed by powder X-ray diffraction (PXRD) patterns (Figure S1 and Figure S2 in the Supporting Information). The polymeric structure of **P1** and the molecular structure of dinuclear complex **2AgNDI** with the atom-numbering scheme are shown in Figure 1. X-ray structural analyses of **P1** and **2AgNDI** reveal that the Ag(I) centers are two-coordinated by two nitrogen atoms from two adjacent NDI dianions in **P1** and one NDI dianion and one ammonia molecule in **2AgNDI** showing the same linear coordination geometry. The Ag−N bond length in **P1** is 2.102(4) Å, and those in **2AgNDI** are 2.103(5) and 2.105(5) Å, while the coordination angles of N1−Ag−N1A ($-x$, $-y$, $2 - z$) are 180° in **P1** and 174.7(2)° in **2AgNDI**. Every NDI unit acts as a bidentate bridging ligand linking neighboring Ag(I) ions to form a 1D coordination polymer in **P1** (Figure 1a) and a dinuclear complex in **2AgNDI**. The adjoining Ag(I)···Ag(I) distances are very similar, being 11.283(2) and 11.288(9) Å in **P1** and **2AgNDI**, respectively.


dx.doi.org/10.1021/cg300776y | Cryst. Growth Des. 2012, 12, 4580−4587

**Table 2. Selected Bond Distances (Å) and Angles (deg) in Complexes 2AgNDI and P1−P5**

| bond distances | | bond angles | |
|---|---|---|---|
| | | **2AgNDI** | |
| Ag1−N1 | 2.103(5) | N1−Ag1−N2 | 174.7(2) |
| Ag1−N2 | 2.105(5) | Ag1−N1−C1 | 114.2(3) |
| | | Ag1−N1−C2 | 123.0(3) |
| | | **P1**[a] | |
| Ag1−N1 | 2.102(4) | N1−Ag1−N1A | 180.0 |
| | | Ag1−N1−C1 | 120.3(3) |
| | | Ag1−N1−C2 | 117.1(3) |
| | | **P2**[a] | |
| Zn1−N1 | 2.043(2) | N1−Zn1−N2 | 106.0(1) |
| Zn1−N2 | 2.040(3) | N1−Zn1−N3 | 104.8(1) |
| Zn1−N3 | 2.025(3) | N1−Zn1−N1A | 129.8(1) |
| | | N2−Zn1−N3 | 102.2 (2) |
| | | **P3**[a] | |
| Cd1−N1 | 2.173(2) | N1−Cd1−N2 | 106.3(1) |
| Cd1−N2 | 2.271(3) | N1−Cd1−N3 | 105.7(1) |
| Cd1−N3 | 2.216(3) | N1−Cd1−N1A | 129.3(1) |
| | | N2−Cd1−N3 | 99.9(2) |
| | | **P4**[a] | |
| Co1−N1 | 2.041(3) | N1−Co1−N2 | 104.9(1) |
| Co1−N2 | 2.056(3) | N1−Co1−N3 | 104.6(2) |
| Co1−N3 | 2.035(4) | N1−Co1−N1A | 132.6(2) |
| | | N2−Co1−N3 | 101.4(2) |
| | | **P5**[a] | |
| Ni1−N1 | 1.906(2) | N1−Ni1−N1A | 180.0 |
| Ni1−N2 | 1.916(3) | N1−Ni1−N2 | 90.0 |
| | | Ni1−N1−C1 | 118.4(2) |

[a]Symmetry codes: **P1**, $-x, -y, 2-z$; **P2** and **P3**, $x, 1/2-y, z$; **P4**, $x, 3/2-y, z$; **P5**, $-x, 1-y, 1-z$.

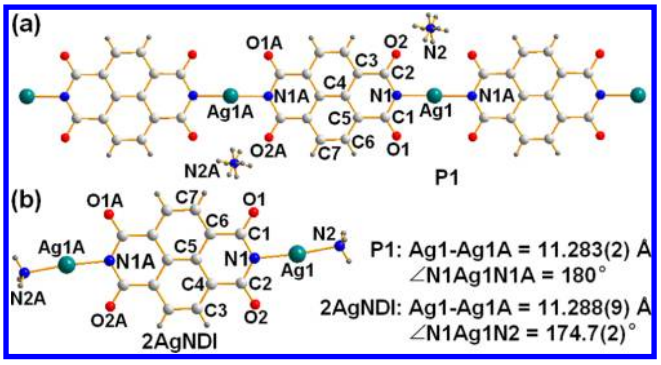


**Figure 1.** Ball-and-stick diagrams of the molecular structures of 1D coordination polymer **P1** (a) and dinuclear complex **2AgNDI** (b) where the distances of Ag···Ag and the coordination angles are shown.

It should be mentioned that all the NDI molecular planes are parallel in **P1** and the quaternary ammonium counterions ($NH_4^+$) play important roles in linking contiguous 1D coordination polymers by N−H···O hydrogen bonds between ammonium and four oxygen atoms of neighboring NDI dianions (Figure 2). Furthermore, they are connected by means of interpolymeric Ag(I)···Ag(I) and face-to-face $\pi-\pi$ stacking interactions between adjacent aromatic rings. It is noted that the shortest interchain Ag(I)···Ag(I) distance is 3.784(6) Å in **P1** and the centroid−centroid separations are 3.784(6) and 3.996(6) Å (Figure 2), forming a condensely packed 3D framework.

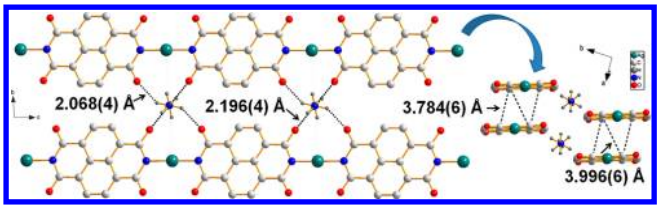


**Figure 2.** Perspective view of the packing structure of 1D coordination polymer **P1**, together with the hydrogen bonds and $\pi-\pi$ stacking interactions. The shortest Ag(I)···Ag(I) distance is 3.784(6) Å.

With regard to the dinuclear complex **2AgNDI**, the shortest Ag(I)···Ag(I) distance is 3.732(3) Å, while the $\pi-\pi$ centroid−centroid separations between adjacent aromatic rings are 3.686(3) and 3.732(3) Å, respectively, as depicted in Figure 3. By comparing the crystal packing structures, it is found that

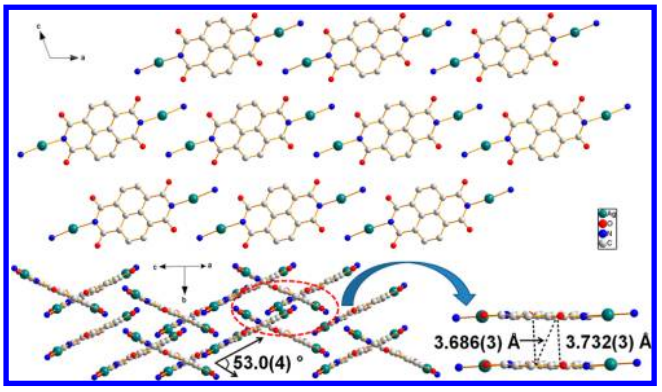


**Figure 3.** Perspective view of the packing structure of dinuclear complex **2AgNDI**, together with the $\pi-\pi$ stacking interactions. The shortest Ag(I)···Ag(I) distance is 3.732(3) Å.

the herringbone packing (ABAB) is present in **2AgNDI** and there are two sets of molecules arranged with a dihedral angle of 53.0(4)°. In contrast, a layer packing fashion (AAAA) is observed in **P1** with an interlayer contact of 3.438(6) Å.

**Structural Description of $[Zn(NDI)(NH_3)_2]_n$ (P2), $[Cd(NDI)(NH_3)_2]_n$ (P3) and $[Co(NDI)(NH_3)_2]_n$ (P4).** The molecular structures of **P2**−**P4** with the atom-numbering schemes are shown in Figure 4a, and the central zinc(II), cadmium(II) and cobalt(II) atoms lie on the inversion centers. These three complexes are nicely isomorphous wherein different divalent cations are present (Zn(II) in **P2**, Cd(II) in **P3** and Co(II) in **P4**). Every metal center in **P2**−**P4** is four-coordinated by four nitrogen atoms from two different NDI dianions and two ammonia molecules. The coordination geometry of the central

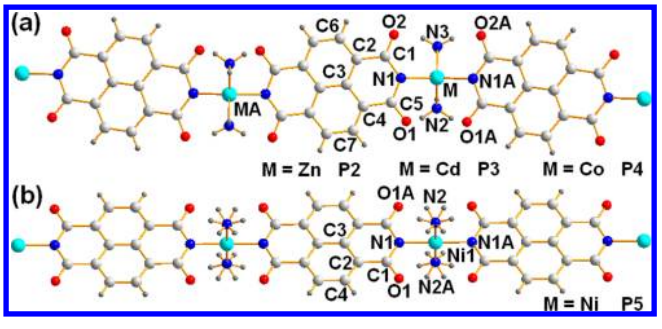


**Figure 4.** Ball-and-stick diagrams of the molecular structures of 1D NDI−M(II) coordination polymer **P2**−**P4** (a) and **P5** (b).


dx.doi.org/10.1021/cg300776y | *Cryst. Growth Des.* 2012, 12, 4580−4587

metal ion is slightly distorted tetrahedral with mean bond lengths of 2.037(3) Å in **P2**, 2.208(2) Å in **P3** and 2.043(3) Å in **P4** due to the dissimilar ionic radii of Zn(II), Cd(II) and Co(II) ions. Different from a straight angle of ∠N−Ag−N in **P1**, the angles of ∠N1−M1−N1A in **P2**−**P4** (**P2** and **P3**, $x$, 1/2 − $y$, $z$; **P4**, $x$, 3/2 − $y$, $z$) are in the range of 129.3(1)−132.6(1)°.

The NDI dianion acts as a bidentate bridging ligand linking contiguous transition-metal centers with similar M(II)···M(II) distances, being 11.105(3), 11.156(3) and 11.107(3) Å in **P2**−**P4**, respectively. As shown in Figure 5, 1D wave-like polymeric

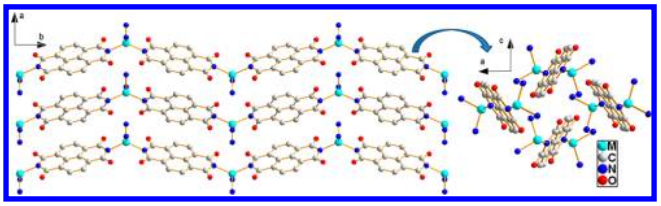

**Figure 5.** Perspective view of packing structure of 1D NDI−M(II) coordination polymer **P2** (M = Zn), **P3** (M = Cd) and **P4** (M = Co).

chains are constructed in **P2**−**P4** where metal ions and planar NDI ligands are alternately arranged. The same ABAB packing mode is found in **P2**−**P4**, and the dihedral angles between the two sets of 1D NDI molecules are 65.8(2), 66.0(2) and 65.9(3)°, respectively.

**Structural Description of $[Ni(NDI)(NH_3)_2]_n$ (P5).** The molecular structure of **P5** with the atom-numbering scheme is shown in Figure 4b. Similar to **P2**−**P4**, single-crystal structural analysis of **P5** reveals that every Ni(II) center is four-coordinated by four nitrogen atoms from two different NDI ligands and two ammonia molecules with a mean Ni(II)−N coordinative bond length of 1.911(3) Å. However, different from the slightly distorted tetrahedral coordination geometry in the cases of **P2**−**P4**, the central Ni(II) ion in **P5** exhibits slightly distorted square planar coordination geometry with zero mean deviation from the least-squares plane. Each NDI dianion serves as a bidentate bridging ligand linking adjoining Ni(II) centers with a Ni(II)···Ni(II) distance of 10.891(3) Å. As depicted in Figure 6, a 1D straight-line polymeric chain

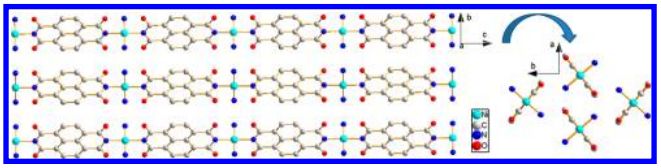

**Figure 6.** Perspective view of the packing structure of 1D NDI−Ni(II) coordination polymer **P5**.

(∠N1−Ni1−N1A = 180°, −$x$, 1 − $y$, 1 − $z$) is formed showing the ABAB packing structure, and the dihedral angle between the two sets of NDI molecules is 75.2(2)°.

**Design, Synthesis and Proposed Formation Mechanism for the Formation of M−NDI Complexes.** The secondary building unit (SBU) has been identified as a useful tool in the synthesis of MCPs. In view of the aforementioned considerations, we simplify the chemical stucture of DPNDI and choose NDI as a building block to self-assemble a series of novel NDI-based metal complexes in this work. Compared with DPNDI, NDI is a more planar, chemically robust and redox-active compound with high melting point and n-type charge mobility, which is an ideal SBU to explore the self-assemblies of versatile $\pi$-conjugated systems. Microcrystal samples of **2AgNDI** and **P1**−**P5** can be easily prepared by heating a mixture of ammonia solution containing different transition-metal salts and NTA at 140 °C for 3 days. However, it is worthwhile to mention that the dark orange and the light orange microcrystals of **P1** and **2AgNDI** are isolated by manual separation (Figure S7 in the Supporting Information).

Different from the interphasial diffusion approach, hydrothermal and solvothermal methods are seldom used in the synthesis of silver(I) complexes mainly because of their thermal instability. In our experiments, we tried to overcome the problem by using a silver(I)−ammonia solution as the starting material, which proved to be a simple and good approach because of its stability under a high-temperature and high-pressure environment compared with the conventional silver(I) salts. In fact, standard electrode potential ($E°$) of $Ag^+/Ag$ (0.80 V) can be significantly decreased to 0.38 V for $[Ag(NH_3)_2]^+/Ag$ species by forming the silver ammonia complex ion. That is to say, the stability of silver ion can be greatly improved in the presence of ammonia. Accordingly, divalent M(II)−ammonia solution [M = Zn(II), Cd(II), Co(II), Ni(II)] can also react with NTA to prepare metal-directed self-assembled complexes.

The synthetic route of **P1** and the proposed formation mechanism are shown in Scheme 3, where the NDI−Ag(I) complexes are chosen as an example. First of all, we try to come up with the simple mechanism based on the single-crystal structures of two important intermediates **2AgNDI** and $NDIH_2$. The reaction begins with the attack of nucleophilic amine on one of the carbonyls of the NTA, which leads to the formation of amic acids and eventually the loss of two water molecules to produce diimide $NDIH_2$. Then 2 equiv of silver ammonia complex ions reacts with $NDIH_2$ forming the dinuclear complex **2AgNDI** and 2 mol of ammonium.

There may be other possible reaction processes. Nevertheless, the ligand-exchange and deprotonated process of $NDIH_2$ are suggested to play important roles in the conversion from $NDIH_2$ to **2AgNDI** and/or mononuclear complex AgNDIH. Furthermore, they are thought to be the rate-determining steps within the reaction.[15] Fortunately, the single crystals of **2AgNDI** as a stable intermediate were obtained from the reaction system. However, the single crystals of AgNDIH could not be isolated, probably owing to its instability. According to the presently available evidence, 1D NDI−Ag(I) coordination polymer **P1** is suggested to be formed step by step.

In fact, the formation of very insoluble silver(I) polymer systems is often one of the driving forces for many reactions. Compared with **2AgNDI** and $NDIH_2$, **P1** shows much lower solubility in commom organic solvents because of its polymeric structure. Actually, we have tried using different stoichiometry and conditions for this reaction in order to get a single product to avoid using manual separation or obtain other intermediates to have a better understanding of the reaction mechanism, but the reaction seems to be more complicated and no other pure products can be isolated successfully. In short, the proposed formation mechanism is simple and somewhat speculative. However, these explanations are mainly based upon the reaction intermediates. Further research is underway on the preparation and formation mechanisms of silver ammonia complexes having some other aromatic-based diimides such as pyromellitic tetracarboxyl diimides and perylene tetracarboxyl diimides.


dx.doi.org/10.1021/cg300776y | *Cryst. Growth Des.* 2012, 12, 4580−4587

**Scheme 3. Synthetic Route of 1D Coordination Polymer P1 and Dinuclear Complex 2AgNDI and Proposed Formation Mechanism**

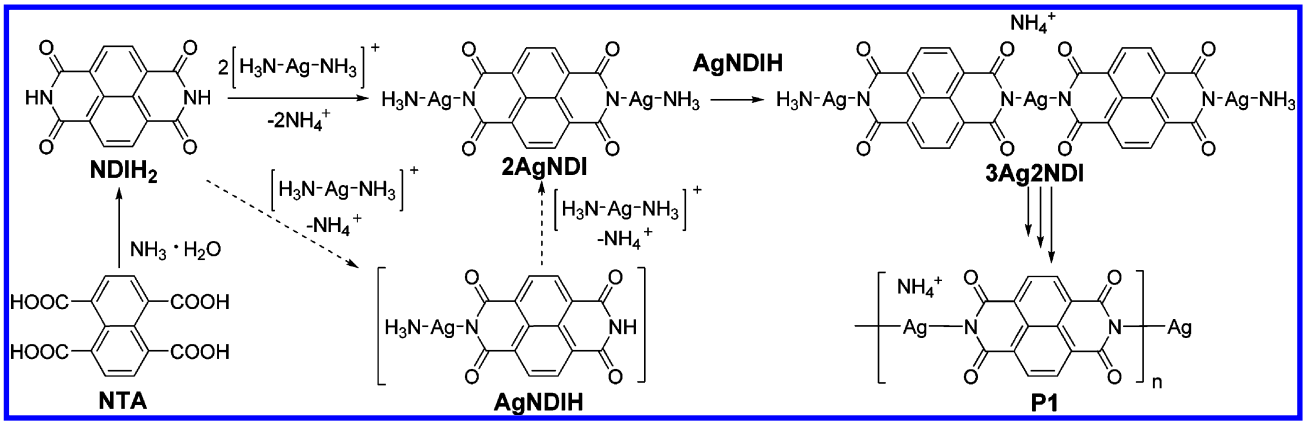


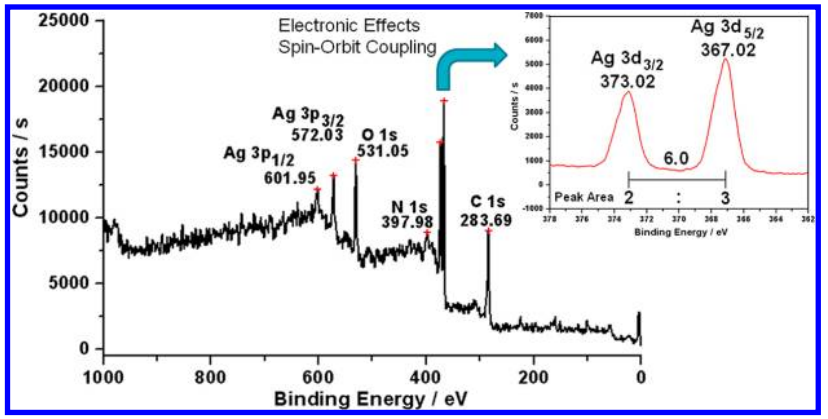


**Figure 7.** XPS spectrum for 1D coordination polymer **P1** with the normal spin−orbit coupling effects (inset).

**XPS Studies.** Considering that a small amount of reduced to Ag(0) atoms, which are undetectable by the X-ray analysis, may well facilitate the color of both **P1** and **2AgNDI** complexes as an impurity of particles of colloidal silver evenly distributed in the mass of the sample, XPS studies for **P1** (Figure 7) and **2AgNDI** (Figure S8 in the Supporting Information) were carried out to further investigate the chemical composition of NDI−Ag(I) complexes. As illustrated in Figure 7 and Figure S8 in the Supporting Information, the spectra clearly reveal the double peaks at 373.02 and 367.02 eV for **P1** and at 373.01 and 366.97 eV for **2AgNDI**, corresponding to the Ag(I) species with the normal spin−orbit coupling effects ($J$ = 6.0 eV) in a peak area ratio of approximately 2:3. At the same time, the characteristic peaks of carbon, hydrogen and nitrogen from NDI ligand can also be found, indicating the correctness of resolving process for two crystal structures.

**Solid-State Conductance Properties.** In this paper, the Ag(I) ion with two-coordinated linear coordination geometry is chosen for the solid-state conductance determination because of its unusual all-parallel-aligned packing structure and abundant Ag···Ag, Ag−$\pi$ and $\pi$−$\pi$ stacking interactions revealed by the aforementioned X-ray analysis.[16] Considering that the solid-state conductance of semiconducting compounds strongly relies on the packing modes of molecules, the solid-state resistivity of single crystals of **P1** and **2AgNDI** has been determined for comparison. Two ends of single-crystal samples of **P1** and **2AgNDI** are covered by a pair of electrodes made of conductive silver paste, and the $I$−$V$ curves are recorded between the pair of electrodes by means of a Lake Shore CRX-4K four-probe system. Linear fitting of the $I$−$V$ curves gave an average resistivity of 7.3 × $10^5$ Ω·m for **P1**, while a control experiment gave an average resistivity of 4.8 × $10^5$ Ω·m for **2AgNDI**, showing the enhancement of solid-state semiconducting conductance (Figure S9 in the Supporting Information). In our previous work,[9e] several linear extensions of bithiophene silver(I) complexes have shown average resistivity on the order of $10^9$ Ω·m magnitude. However, **P1** presents better solid-state semiconducting conductance in this paper, which could be ascribed to the rigid 1D straight-line and planar polymeric structure fixed by N−Ag coordinative bonds, all-parallel-aligned packing structure and Ag(I)···Ag(I) interactions, and strong hydrogen bonds down the crystallogarphic $c$, $a$ and $b$ axes, respectively.

**Theoretic Calculations.** To further reveal the band structures and density of states of **P1** and **2AgNDI** (Figure S10 in the Supporting Information), density functional calculations were carried out using the generalized gradient approximation (GGA) Perdew, Burke, and Ernzerhof (PBE) functional[17] implemented in the Cambridge Sequential Total Energy Package (CASTEP).[18] The convergence criteria for the structural optimization were set to an energy tolerance of 1.0 × $10^{-5}$ eV/atom together with a maximum force of 0.03 eV/Å on each atom and a maximum displacement of 1.0 × $10^{-3}$ Å. We used 4 × 2 × 2 Monkhorst−Pack meshes for the sampling of the Brillouin zone of **P1**, and gamma point for the calculation of **2AgNDI**. Ultrasoft pseudopotentials[19] were used to describe the ionic cores; the Kohn−Sham one-electron states were expanded in a plane wave basis with a cutoff energy of 340 eV.


dx.doi.org/10.1021/cg300776y | Cryst. Growth Des. 2012, 12, 4580−4587

The resultant band gaps for **P1** and **2AgNDI** are 1.72 and 2.04 eV, respectively, which are in agreement with their solid-state semiconducting conductance. Figure S11 in the Supporting Information gives the frontier molecular orbitals of NDI for comparison (showing a band gap of 3.88 eV), from which one can see the obvious decrease of band gaps from NDI to **P1** after Ag(I) ion complexation.

## CONCLUSION

In summary, we have reported herein a series of novel linear naphthalenediimidato-based MCPs, which is the first structural report on the preparation and structures of metal−naphthalenediimidato complexes. Metal-directed assembly of NTA with different transition-metal salts in the presence of ammonia exhibits distinguishable 1D coordination polymers with highly symmetrical NDI ligands. It is worth noting that the 1D straight-line NDI−Ag(I) coordination polymer **P1** is formed stepwise from a dinuclear intermediate **2AgNDI**, and it exhibits an unusual all-parallel-aligned packing structure (AAAA) which is different from the ABAB packing mode for **P2**−**P5** and **2AgNDI**. Solid-state conductance studies for **P1** reveal it has good semiconducting properties, of which the result is in agreement with that of theoretic calculations by the density functional theory combined with ultrasoft pseudopotentials. Ammonia is present in the synthesis serving as a stabilizing reagent of Ag(I) ion and a weak base to remove the protons of $NDIH_2$ simultaneously. Our results strongly suggest that the NDI units can be successfully designed for use in the solid-state conductive devices and further demonstrate the promising performance of single-crystal OFETs.

## ASSOCIATED CONTENT

### Supporting Information

X-ray crystallographic data in CIF format for **2AgNDI** and **P1**−**P5**, hydrogen-bonding interactions, simulative and experimental PXRD diagrams, microcrystal photos, XPS analysis, linear fitting of the *I*−*V* curves and computational details for related complexes. This material is available free of charge via the Internet at http://pubs.acs.org. CCDC numbers 867654, 867655 and 885026−885029 for **2AgNDI** and **P1**−**P5** contain the supplementary crystallographic data of the metal complexes. These data can also be obtained free of charge, upon request, at www.ccdc.cam.ac.uk/conts/retrieving.html [or from the Cambridge Crystallographic Data Centre, 12 Union Road, Cambridge CB2 1EZ, U.K.; fax (Internet) +44−1223/336−033; e-mail request@ccdc.cam.ac.uk].

## AUTHOR INFORMATION

### Corresponding Author

*Tel: +86-25-83686526. Fax: +86-25-83314502. E-mail: whuang@nju.edu.cn; zxchen@nju.edu.cn.

### Notes

The authors declare no competing financial interest.

## ACKNOWLEDGMENTS

We acknowledge the Major State Basic Research Development Program (No. 2011CB933300 and No. 2011CB808704) and the National Natural Science Foundation of China (No. 21171088 and No. 21021062) for financial aid.

## REFERENCES

(1) (a) Chisholm, M. H. *Acc. Chem. Res.* **2000**, *33*, 53−61. (b) Zheng, S. L.; Tong, M. L.; Chen, X. M. *Coord. Chem. Rev.* **2003**, *246*, 185−202. (c) De Cola, L. *Molecular Wires*; Springer: 2005; (d) Zeng, Y. F.; Hu, X.; Liu, F. C.; Bu, X. H. *Chem. Soc. Rev.* **2009**, *38*, 469−480. (e) Chakrabarty, R.; Mukherjee, P. S.; Stang, P. J. *Chem. Rev.* **2011**, *111*, 6810−6918. (f) Leong, W. L.; Vittal, J. J. *Chem. Rev.* **2011**, *111*, 688−764. (g) Torrent, M. M.; Rovira, C. *Chem. Rev.* **2011**, *111*, 4833−4856.

(2) (a) Benniston, A. C.; Harriman, A.; Rewinska, D. B.; Yang, S. J.; Zhi, Y. G. *Chem.—Eur. J.* **2007**, *13*, 10194−10203. (b) Knudsen, M. M.; Kalashnyk, N.; Masini, F.; Cramer, J. R.; Laegsgaard, E.; Besenbacher, F.; Linderoth, T. R.; Gothelf, K. V. *J. Am. Chem. Soc.* **2011**, *133*, 4896−4905. (c) Grunder, S.; Torres, D. M.; Marquardt, C.; Błaszczyk, A.; Krupke, R.; Mayor, M. *Eur. J. Org. Chem.* **2011**, 478−496. (d) Duan, X. Y.; Meng, Q. J.; Su, Y.; Li, Y. Z.; Duan, C. Y.; Ren, X. M.; Lu, C. S. *Chem.—Eur. J.* **2011**, *17*, 9936−9943.

(3) (a) Chan, C. K. M.; Tao, C. H.; Li, K. F.; Wong, K. M. C.; Zhu, N. Y.; Cheah, K. W.; Yam, V. W. W. *Dalton Trans.* **2011**, *40*, 10670−10685. (b) Yeung, M. C. L.; Yam, V. W. W. *Chem.—Eur. J.* **2011**, *17*, 11987−11990. (c) Wong, H. L.; Tao, C. H.; Zhu, N. Y.; Yam, V. W. W. *Inorg. Chem.* **2011**, *50*, 471−481. (d) Lo, W. Y.; Lam, C. H.; Yam, V. W. W.; Zhu, N. Y.; Cheung, K. K.; Fathallah, S.; Messaoudi, S.; Le, G. B.; Kahlal, S.; Halet, J. F. *J. Am. Chem. Soc.* **2004**, *126*, 7300−7310. (e) Wong, K. M. C.; Hui, C. K.; Yu, K. L.; Yam, V. W. W. *Coord. Chem. Rev.* **2002**, *229*, 123−132. (f) Yam, V. W. W.; Chong, S. H. F.; Ko, C. C.; Cheung, K. K. *Organometallics* **2000**, *19*, 5092−5097. (g) Yam, V. W. W.; Li, C. K.; Chan, C. L. *Angew. Chem., Int. Ed.* **1998**, *37*, 2857−2859.

(4) (a) Berenguer, J. R.; Bernechea, M.; Fernandez, J.; Gil, B.; Lalinde, E.; Moreno, M. T.; Ruiz, S.; Sanchez, S. *Organometallics* **2011**, *30*, 4665−4677. (b) Diez, A.; Fornies, J.; Gomez, J.; Lalinde, E.; Martin, A.; Moreno, M. T.; Sanchez, S. *Dalton Trans.* **2007**, *33*, 3653−3660. (c) Berenguer, J. R.; Gil, B.; Fernandez, J.; Fornies, J.; Lalinde, E. *Inorg. Chem.* **2009**, *48*, 5250−5262. (d) Fornies, J.; Fuertes, S.; Martin, A.; Sicilia, V.; Gil, B.; Lalinde, E. *Dalton Trans.* **2009**, *12*, 2224−2234. (e) Diez, A.; Fernandez, J.; Lalinde, E.; Moreno, M. T.; Sanchez, S. *Dalton Trans.* **2008**, *36*, 4926−4936.

(5) (a) Pan, M.; Lin, X.-M.; Li, G.-B.; Su, C.-Y. *Coor. Chem. Rev.* **2011**, *255*, 1921−1936. (b) Mulfort, K. L.; Farha, O. K.; Malliakas, C. D.; Kanatzidis, M. G.; Hupp, J. T. *Chem.—Eur. J.* **2010**, *16*, 276−281. (c) Farha, O. K.; Malliakas, C. D.; Kanatzidis, M. G.; Hupp, J. T. *J. Am. Chem. Soc.* **2010**, *132*, 950−952. (d) Furukawa, S.; Hirai, K.; Takashima, Y.; Nakagawa, K.; Kondo, M.; Tsuruoka, T.; Sakata, O.; Kitagawa, S. *Chem. Commun.* **2009**, 5097−5099. (e) Dinolfo, P. H.; Williams, M. E.; Stern, C. L.; Hupp, J. T. *J. Am. Chem. Soc.* **2004**, *126*, 12989−13001. (f) Ma, B.-Q.; Mulfort, K. L.; Hupp, J. T. *Inorg. Chem.* **2005**, *44*, 4912−4914. (g) Takashima, Y.; Martnez, V. M.; Furukawa, S.; Kondo, M.; Shimomura, S.; Uehara, H.; Nakahama, M.; Sugimoto, K.; Kitagawa, S. *Nat. Commun.* **2011**, *2*, 168−175. (h) Chung, H.; Barron, P. M.; Novotny, R. W.; Son, H.-T.; Hu, C.-H.; Choe, W.-Y. *Cryst. Growth Des.* **2009**, *9*, 3327−3332. (i) Nelson, A. P.; Parrish, D. A.; Cambrea, L. R.; Baldwin, L. C.; Trivedi, N. J.; Mulfort, K. L.; Farha, O. K.; Hupp, J. T. *Cryst. Growth Des.* **2009**, *9*, 4588−4591.

(6) (a) Hutchison, G. R.; Ratner, M. A.; Marks, T. J. *J. Am. Chem. Soc.* **2005**, *127*, 2339−2350. (b) Coropceanu, V.; Cornil, J.; Da Silva Filho, D. A.; Olivier, Y.; Silbey, R.; Bredas, J. L. *Chem. Rev.* **2007**, *107*, 926−952 and references therein.

(7) (a) Amabilino, D. B.; Stoddart, J. F. *Chem. Rev.* **1995**, *95*, 2725−2828. (b) Bhosale, S. V.; Jania, C. H.; Langford, S. J. *Chem. Soc. Rev.* **2008**, *37*, 331−342.

(8) (a) Wurthner, F.; Ahmed, S.; Thalacker, C.; Debaerdemaeker, T. *Chem.—Eur. J.* **2002**, *8*, 4742−4750. (b) Miller, L. L.; Duan, R. G.; Hong, Y.; Tabakovic, I. *Chem. Mater.* **1995**, *7*, 1552. (c) Vicic, D. A.; Odom, D. T.; Nunez, M. E.; Gianolio, D. A.; McLaughlin, L. W.; Barton, J. K. *J. Am. Chem. Soc.* **2000**, *122*, 8603−8611. (d) Lee, H. N.; Xu, Z.; Kim, S. K.; Swamy, K. M. K.; Kim, Y.; Kim, S. J.; Yoon, J. *J. Am. Chem. Soc.* **2007**, *129*, 3828−3829.

(9) (a) Huang, W.; Masuda, G.; Maeda, S.; Tanaka, H.; Hino, T.; Ogawa, T. *Inorg. Chem.* **2008**, *47*, 468−480. (b) Wang, L.; You, W.; Huang, W.; Wang, C.; You, X. Z. *Inorg. Chem.* **2009**, *48*, 4295−4305. (c) Huang, W.; Wang, L.; Tanaka, H.; Ogawa, T. *Eur. J. Inorg. Chem.* **2009**, 1321−1330. (d) Hu, B.; Xu, F.; Fu, S. J.; Tao, T.; Wang, Y. N.; Huang, W. *Inorg. Chim. Acta* **2010**, *363*, 1348−1354. (e) Wang, L.; Tao, T.; Fu, S. J.; Wang, C.; Huang, W.; You, X. Z. *CrystEngComm* **2011**, *13*, 747−749. (f) Hu, B.; Fu, S. J.; Xu, F.; Tao, T.; Zhu, H. Y.; Cao, K. S.; Huang, W.; You, X. Z. *J. Org. Chem.* **2011**, *76*, 4444−4456.
(10) (a) Huang, W.; Masuda, G.; Maeda, S.; Tanaka, H.; Ogawa, T. *Chem.—Eur. J.* **2006**, *12*, 607−619. (b) Huang, W.; Tanaka, H.; Ogawa, T. *J. Phys. Chem. C* **2008**, *112*, 11513−11526. (c) Huang, W.; Tanaka, H.; Ogawa, T.; You, X. Z. *Adv. Mater.* **2010**, *22*, 2753−2758.
(11) (a) Perron, J.; Beauchamp, A. L. *Inorg. Chem.* **1984**, *23*, 2853−2859. (b) Treichel, P. M.; Nakagaki, P. C.; Haller, K. J. *J. Organomet. Chem.* **1987**, *327*, 327−337. (c) Falvello, L. R.; Pascual, I.; Tomas, M.; Urriolabeitia, E. P. *J. Am. Chem. Soc.* **1997**, *119*, 11894−11902. (d) Savjani, N.; Lancaster, S. J.; Bew, S.; Hughes, D. L.; Bochmann, M. *Dalton Trans.* **2011**, *40*, 1079−1090. (e) Chaignon, N. M.; Fairlamb, I. J. S.; Kapdi, A. R.; Taylor, R. J. K.; Whitwood, A. C. *J. Mol. Catal. A: Chem.* **2004**, *219*, 191−199. (f) Fairlamb, I. J. S.; Kapdi, A. R.; Lynam, J. M.; Taylor, R. J. K.; Whitwood, A. C. *Tetrahedron* **2004**, *60*, 5711−5718. (g) Ruiz, J.; Vicente, C.; Cutillas, N.; Perez, J. *Dalton Trans.* **2005**, 1999−2006.
(12) Siemens. *SAINT v4 software reference manual*; Siemens Analytical X-ray Systems, Inc.: Madison, WI, USA; 2000.
(13) Sheldrick, G. M. *SADABS, program for empirical absorption correction of area dectector data*; Univ. of Gottingen: Germany; 2000.
(14) Siemens. *SHELXTL, Version 6.10 reference manual*; Siemens Analytical X-ray Systems, Inc.: Madison, Wisconsin, USA; 2000.
(15) Bruno, P. *Tomorrow's Chemistry Today: Concepts in Nanoscience, Organic Materials and Environmental Chemistry*, 2nd ed.; WILEY-VCH Verlag GmbH & Co. KGaA: Weinheim, 2009.
(16) (a) Blake, A. J.; Champness, N. R.; Hubberstey, P.; Li, W. S.; Withersby, M. A.; Schroder, M. *Coord. Chem. Rev.* **1999**, *183*, 117−138. (b) Khlobystov, A. N.; Blake, A. J.; Champness, N. R.; Lemenovskii, D. A.; Majouga, A. G.; Zyk, N. V.; Schroder, M. *Coord. Chem. Rev.* **2001**, *222*, 155−192. (c) Shimizu, G. K. H.; Enright, G. D.; Ratcliffe, C. I.; Ripmeester, J. A.; Wayner, D. D. M. *Angew. Chem., Int. Ed.* **1998**, *37*, 1407−1409. (d) Omary, M. A.; Webb, T. R.; Assefa, Z.; Shankle, G. E.; Patterson, H. H. *Inorg. Chem.* **1998**, *37*, 1380−1386.
(17) Perdew, J. P.; Burke, K.; Ernzerhof, M. *Phys. Rev. Lett.* **1996**, *77*, 3865−3868.
(18) Milman, V.; Winkler, B.; White, J. A.; Pickard, C. J.; Payne, M. C.; Akhmataskaya, E. V.; Nobes, R. H. *Int. J. Quantum Chem.* **2000**, *77*, 895−910.
(19) Vanderbilt, D. *Phys. Rev. B* **1990**, *41*, 7892−7895.